Possibility of determining parameters of size spectra and flutter of crystal plates from data of monostatic and bistatic laser sensing

O.V. Shefer

Tomsk State University
Institute of Atmospheric Optics,
Siberian Branch of the Russian Academy of Sciences, Tomsk

Received February 11, 2003

The information borne by the characteristics of reflected optical radiation in the cases of single- or double-ended lidar is studied within the framework of a crystal cloud model as a system of oriented crystal plates. Advantages of the double-ended or bistatic laser sensing technique over the single-ended or monostatic one are noticed. It is shown that the variation of the absolute and relative values of the scattering coefficient obtained at small-angle scanning carries the information about the size spectrum of crystal plates and their flutter in atmospheric formations with inhomogeneous composition.

Introduction

As known, natural ice clouds mostly consist of oriented particles.[1] The position of crystals in space depends on the air mass motion and is determined by the difference between the falling-down velocity vector and the wind velocity vector. The most stable position is apparently characteristic of crystals with extended shapes. However, they flutter about the plane of their dominant orientation. It was found experimentally that in calm atmospheric layers the flutter of plates and columns does not exceed 1 deg (Refs. 2 and 3). In moving layers (in particular, cloud bottom) the particle flutter is about 5–10°. It should be noted that plates along with crystals of other shapes have both the smallest flutter[4] and the largest area of the plane surface, which forms the maximum directed flux of the reflected energy.[2] These particles are a kind of a mirror. As to hexagonal plates, they also have plane sides, but the intensity of radiation reflected from them decreases considerably due to revolution about the maximum axis. Besides, the percentage of plate crystals in an ice cloud often prevails over the fractions of particles having other habits. Therefore, just plates apparently give the largest contribution to formation of high-intensity reflected radiation. In particular, specular reflection of optical radiation leads to formation of the so-called abnormal backscattering.[2,3]

Optical methods are now widely used to study crystal clouds, and bistatic laser sensing is distinguished by its advantages among these methods.[5] In Ref. 6 for an ensemble of horizontally oriented ice plates we analyzed the information content of the ratio of backscattering coefficients, one of which was obtained at the vertical position of the lidar axis and the other – at its small deviation from the vertical. It was also shown there that the size spectrum and flutter of plates can be estimated from the data of monostatic laser sensing. However, interpretation of the data of abnormal backscattering may face difficulties connected with the absence of *a priori* information. In particular, the deficit of additional information about the cloud composition and particle orientation does not allow the intensities caused by specular reflection of radiation just from plates to be correctly separated out from the data of monostatic sensing.

It should be taken into account that the high-amplitude echo signal can be formed at reflection from large (size of hundreds and thousands of micrometers) spherical particles or plane sides of hexagonal columns. Besides, both at specular reflection from plates and from spherical particles, the state of polarization of the incident radiation does not change. However, all the difficulties in analysis associated with the above uncertainty for the case of monostatic sensing are removed when we pass on to the bistatic scheme. In sensing crystal clouds with such a lidar, a receiver can record the maximum possible intensity of the specularly reflected signal along with particular polarization characteristics inherent in a certain type of particles. This allows us to exclude the uncertainty in analysis of sensing data for even atmospheric formations with a complicated structure. Moreover, an advantage of the bistatic sensing over the monostatic one is that unites two requirements that are contradictory in the scheme, in which the source and receiver are matched.

In monostatic sensing, on the one hand, the echo signal with the abnormally high amplitude should be recorded to estimate the crystal cloud microstructure parameters, and, on the other hand, it should be taken into account that polarization characteristics (in particular, depolarization ratio) carry more information about the orientation of crystals and

0235-6880/03/04 318-07 $02.00

their refractive index, if the lidar axis is strongly deflected from the vertical, and, consequently, the echo signal is weaker. The receiver of a bistatic polarization lidar at specular reflection of radiation can detect high-amplitude polarized signal carrying complete information about optical, orientation, and microphysical properties of a crystal cloud sounded.

In Ref. 7 we presented a numerical model of a plate as applied to bistatic polarization laser sensing, which included a particular case of single-ended lidar sensing arrangement. As applied to monostatic sensing, we revealed that the scattering characteristics bear the information sought and developed the schemes for determination of the refractive index, orientation, and size spectrum of plates.[6,8] In this connection, it should be expected that similar methods for estimation of the physical parameters of crystals can be used for bistatic sensing as well. In this case, some peculiarities may arise due to more complex angular dependences, including, first of all, orientation of the polarization plane of the incident radiation with respect to a scatterer and the receiver.

Relationship between the positions of source, receiver, and scatterer as applied to bistatic sensing scheme

The angular characteristics needed in the bistatic sensing scheme for numerical determination of the field scattered by the system of oriented plates fluttering about some stable positions are shown in Fig. 1.

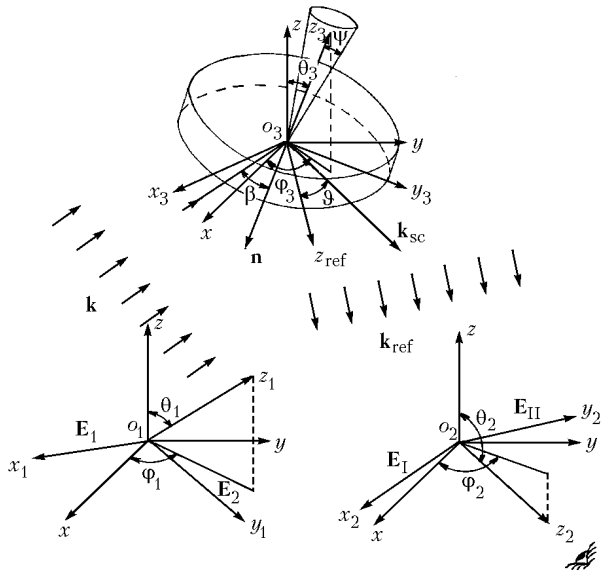

Fig. 1. Scheme of bistatic laser sensing.

Assume that the source of radiation is located at the point o_1, the receiver is at the point o_2, the object under study is at the point o_3, and $oxyz$ is the absolute coordinate system, with respect to which three coordinate systems more are introduced: $o_1x_1y_1z_1$, $o_2x_2y_2z_2$, and $o_3x_3y_3z_3$ that are associated, respectively, with the source, the receiver, and the scatterer. The coordinate plane oxy is parallel to the ground, and the normal to it is directed along the oz axis. The propagation of the sounding radiation coincides with the positive direction of the o_1z_1 axis. The wave vector $\mathbf{k}$ indicates the direction of propagation of the incident radiation. It is obvious that $\mathbf{k} \parallel o_1z_1$. Electric components of the incident wave of elliptic polarization $(\mathbf{E}_1, \mathbf{E}_2)$ are directed along the axes o_1x_1 and o_1y_1.

As a scatterer, we selected a system of identically oriented plates. The plane parallel to plate bases will be called the plane of preferred orientation. This plane will be denoted as $o_3x_3y_3$ and taken as a coordinate plane. The angle β is the angle between the direction of sensing $\mathbf{k}$ (or the axis o_1z_1) and the normal to the plate base $\mathbf{n}$ (or the axis o_3z_3). The rays specularly reflected from the plate base or coming out after a series of internal re-reflections, are formed in the direction o_3z_{ref}, $\mathbf{k}_{\text{ref}}$ is the direction of propagation of the specularly reflected beam, $\mathbf{k}_{\text{ref}} \parallel o_3z_{\text{ref}}$. The elevation angle ψ and the azimuth angle ξ specify possible fluctuations of the plates about the axis o_3z_3. As ξ varies from 0 to 2π and at the given value $\psi' = \psi$, the normal to the plate base describes a cone with the axis o_3z_3. The scattered radiation is received from the direction $\mathbf{k}_{\text{sc}}$ (or the axis o_2z_2), and the axis o_2y_2 is parallel to the horizontal plane (or the ground plane); $\mathbf{E}_{\text{I}}$ and $\mathbf{E}_{\text{II}}$ are the components of the field recorded in the receiver that are directed along the o_2x_2 and o_2y_2 axes, respectively. The deviation of the direction of reception from the line of "strictly" specular reflection (that is, the angle between the directions o_3z_{ref} and $\mathbf{k}_{\text{sc}}$) is denoted as ϑ.

To represent the normalized scattering characteristics, it is sufficient to determine the angular positions of unit vectors specifying the components of the scattered field. For this purpose, let us match the origins of all the four coordinate systems at the same point o and express the unit vectors $(\mathbf{x}, \mathbf{y}, \mathbf{z})$ of the absolute coordinate system through the unit vectors $(\mathbf{x}_i, \mathbf{y}_i, \mathbf{z}_i)$ as:

$$\begin{pmatrix} \mathbf{x} \\ \mathbf{y} \\ \mathbf{z} \end{pmatrix} = S_i \begin{pmatrix} \mathbf{x}_i \\ \mathbf{y}_i \\ \mathbf{z}_i \end{pmatrix}, \quad i = 1, 2, 3,$$

where

$$S_i = \begin{pmatrix} \cos\varphi_i \cos\vartheta_i & -\sin\varphi_i & \cos\varphi_i \sin\vartheta_i \\ \sin\varphi_i \cos\vartheta_i & \cos\varphi_i & \sin\varphi_i \sin\vartheta_i \\ -\sin\vartheta_i & 0 & \cos\vartheta_i \end{pmatrix}.$$

The angles ϑ_i and φ_i apparently determine the positions of the basis vectors $\mathbf{x}_i$, $\mathbf{y}_i$, $\mathbf{z}_i$ $(i = 1, 2, 3)$ for each of the three corresponding coordinate systems $ox_iy_iz_i$ $(i = 1, 2, 3)$ relative to the absolute system $oxyz$.

Formulation of the problem

Let we have some plate-shaped crystals. The particle size spectrum is described by the gamma distribution function[9]:

$$N(a) = N \frac{\mu^{\mu+1}}{\Gamma(\mu+1)} \frac{1}{a_m} \left(\frac{a}{a_m}\right)^{\mu} e^{-\mu a/a_m}, \qquad (1)$$

where N is the concentration of plates; a_m is the plate radius corresponding to the maximum of the function $N(a)$; μ is a dimensionless parameter characterizing how steep is the slope of this maximum; Γ is the gamma function. Note that the mean plate radius $\overline{a}$ is related to a_m as[10]:

$$\overline{a} = a_m(1 + 1/\mu). \qquad (2)$$

Particles have the complex refractive index $\tilde{n} = n + i\chi$.

The system of oriented plates fluttering about their stable position is exposed to optical radiation, which is reflected specularly from plate bases. Determine the scattering coefficient for the specularly reflected radiation when the radiation source and the receiver are spatially separated.

The equations for the scattering coefficients in the backward hemisphere were obtained in Ref. 10 assuming that the plates are strictly oriented in space. Note that the backward hemisphere is that part of the sphere, which is bounded by the plate base and includes the incident and reflected rays. In this connection, the subscript π is introduced in designations of the corresponding scattering characteristics. The integral representation for the scattering coefficients has the form

$$\beta_{\pi_i} = \int N(a)\sigma_{\pi_i} da \quad (i = 1, 2, 3, 4), \qquad (3)$$

where β_{π_i} are the scattering coefficients proportional to the corresponding parameters of the Stokes vector; $N(a)$ is the particle size distribution function (1), σ_{π_i} $(i = 1, 2, 3, 4)$ are scattering cross sections. The equations for σ_{π_i} were derived in Ref. 7 within the framework of physical optics.

Under natural conditions, the crystals are known to flutter about their stable position. Let us now determine, for an ensemble of ice plates, taking into account their possible flutter, the scattering coefficient proportional to the intensity of specularly reflected radiation. The flutter angle will be described by two parameters (ψ', ξ), where ψ' is the height angle and ξ is the azimuth angle, which determine possible deviations of the plate normal from the o_3z_3 axis (see Fig. 1). Let the two-dimensional random parameter (ψ', ξ) be uniformly distributed over a solid angle bounded by a conical surface, where $\xi \in [0, 2\pi]$ and $\psi' \in [0, \psi]$. Numerical calculations showed that variation of the amplitude of the reflected signal at possible plate fluttering is mostly determined by the parameter ψ. Besides, this is confirmed by analysis of the corresponding azimuth dependences presented in Refs. 10 and 11. To decrease the computational time for the needed characteristics (without loss of accuracy), it is sufficient to perform averaging only over the elevation angle ψ'. For this purpose, the function $\beta_{\pi_i}(x)$ should be integrated over the range $[-\psi; \psi]$. As a result, we obtain

$$\beta_F(\psi) = \frac{1}{2\psi} \int_{-\psi}^{\psi} \beta_{\pi_1}(x)dx . \qquad (4)$$

Thus, Eq. (4) determines the scattering coefficient for the specularly reflected radiation, when the source and the receiver are spatially separated in the case of fluttering ice plates.

The deviation of the reception direction from the line of strictly specular reflection (angle ϑ) leads to the shift of the integration range by the same value. As a result, the coefficient $\beta_F(\psi, \vartheta)$ is determined through averaging of the function $\beta_{\pi_i}(x)$ over the range $[-\psi + \vartheta; \psi + \vartheta]$, that is,

$$\beta_F(\psi, \vartheta) = \frac{1}{2\psi} \int_{-\psi+\vartheta}^{\psi+\vartheta} \beta_{\pi_1}(x)dx . \qquad (5)$$

In experimental investigation of clouds including horizontally oriented plates, the sharp change of the amplitude of the received signal was observed at lidar scanning within 1° (Ref. 3). In Ref. 10 we showed that in the case of specular reflection at bistatic sensing of a disperse medium including oriented plates the deflection of the reception axis by only 1° decreases the amplitude of the recorded signal by several orders of magnitude (as compared with the case of $\vartheta = 0°$). Note that these changes of the echo signal are observed at any angle β of the radiation incidence onto the plate. When studying the scattering coefficient $\beta_{\pi_i}(\vartheta)$ in the backward hemisphere, it is of prime interest its behavior in the range of small ϑ angles. The same conclusion can be drawn from analysis of the ratio of the scattering coefficients $\beta_F(\psi, \vartheta)/\beta_F(\psi, 0)$ for the system of fluttering crystals. It should be noted that the condition of a small (no larger than 1°) angle should be fulfilled for the sum of angles $\psi + \vartheta$. The ratios $\beta_{\pi_1}(\vartheta)/\beta_{\pi_1}(0)$ and $\beta_F(\psi, \vartheta)/\beta_F(\psi, 0)$ are apparently independent of the concentration of plates in the scattering volume, since N enters as a factor into both the numerator and denominator of these ratios.

Discussion of numerical calculations

Let us analyze the characteristics of reflected radiation, which are interesting for bistatic laser sensing. For this purpose let us use Eqs. (3)–(5). In all the calculations presented below, linear

polarization of the incident field is taken for certainty.

Figure 2 depicts the dependence of the ratio $\beta_{\pi_1}(\vartheta)/\beta_{\pi_1}(0)$ on the angle ϑ at different parameters $\overline{a}$ and μ for an ensemble of strictly oriented ice plates (i.e., $\psi = 0°$). Each area between the curves *1* and *2*, *3* and *4*, *5* and *6*, *7* and *8* is continuously filled with curves for $\beta_{\pi_1}(\vartheta)/\beta_{\pi_1}(0)$ shifted relative to each other and obtained at different values of μ from the range [1; 10]. The highest value of μ corresponds to the least steep curve. Similar regularities were presented in our Ref. 6 for the case of monostatic laser sensing. The values shown in Fig. 2 were calculated for $\beta = 20°$. Numerical calculations showed that the relative characteristics $\beta_{\pi_1}(\vartheta)/\beta_{\pi_1}(0)$ and $\beta_F(\psi, \vartheta)/\beta_F(\psi, 0)$ do not change at variations of β, but depend mostly on μ and $\overline{a}$. As the parameter μ increases, the number of plates having the radii larger than the mean value decreases. Comparing the corresponding two curves belonging to different ranges in Fig. 2, we can see that the plates with a smaller base give the lower steepness of the characteristic $\beta_{\pi_1}(\vartheta)/\beta_{\pi_1}(0)$. Besides, in the range of small angles ϑ the rate of change of the $\beta_{\pi_1}(\vartheta)/\beta_{\pi_1}(0)$ curve is determined, to a higher extent, by the mean plate radius $\overline{a}$ and, to the lower extent, by the μ parameter. For the case of bistatic sensing using specular reflection, at small-angle lidar (or source) scanning, the variation of reflected radiation can give the information on the mean plate radius even at unknown distribution parameter μ. However, the accuracy of determination of the parameter $\overline{a}$ increases considerably, if the parameter μ takes values from the range less than [1; 10].

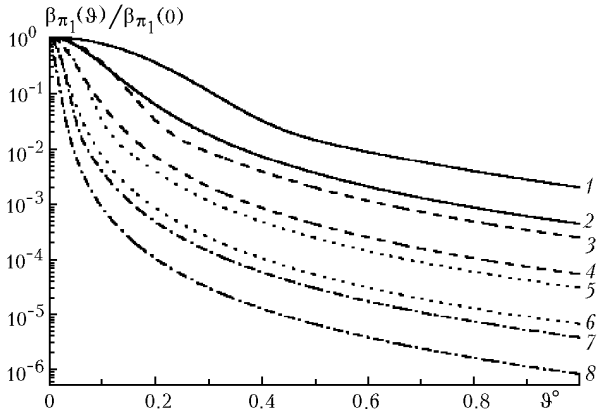

Fig. 2. Dependence of the ratio of scattering coefficients $\beta_{\pi_1}(\vartheta)/\beta_{\pi_1}(0)$ for a system of strictly oriented plates: $\theta_1 = -40°$, $\varphi_1 = 0°$, $\theta_2 = 100°$, $\varphi_2 = 0°$, $\beta = 20°$, $\lambda = 0.694$ μm, $\tilde{n} = 1.31 + i\cdot10^{-3}$: $\overline{a} = 25$ μm, $\mu = 1$ (*1*); $\overline{a} = 25$ μm, $\mu = 10$ (*2*); $\overline{a} = 50$ μm, $\mu = 1$ (*3*); $\overline{a} = 50$ μm, $\mu = 10$ (*4*); $\overline{a} = 100$ μm, $\mu = 1$ (*5*); $\overline{a} = 100$ μm, $\mu = 10$ (*6*); $\overline{a} = 200$ μm, $\mu = 1$ (*7*); $\overline{a} = 200$ μm, $\mu = 10$ (*8*).

At a specular reflection of optical radiation from a system of oriented plates, the abnormally high-amplitude signal is formed.[2,3] The detector may be damaged in recording this signal. The high intensity of radiation is caused by stability of identically oriented plates. However, possible plate fluctuations about the plane of the strict orientation decrease the directivity of reflection from an ensemble of crystals as a whole and, consequently, the intensity of the radiation recorded.

Figure 3 depicts the dependence of scattering coefficient for the specularly reflected radiation on the flutter angle ψ, that is, $\beta_F(\psi)$. Even small fluctuations of plates about the strict orientation plane decrease the absolute values of $\beta_F(\psi)$ by one to two orders of magnitude. Nevertheless, the amplitude of reflected field remains abnormally high. The rate of change of $\beta_F(\psi)$ in the range of small ψ (e.g., $\psi \in [0; 0.4]$) is connected with the value of $\overline{a}$. For larger particles, the slopes of $\beta_F(\psi)$ curves are much more steep.

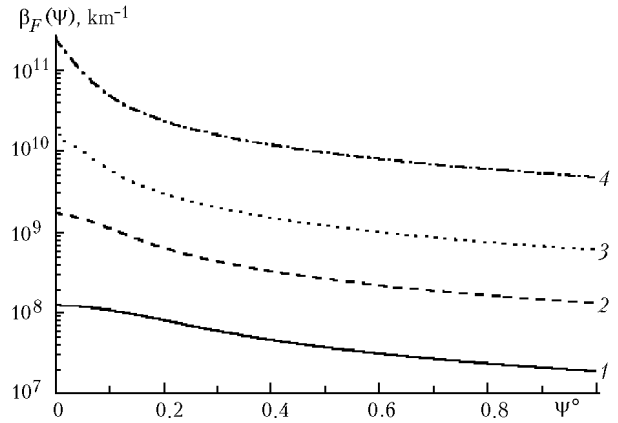

Fig. 3. Scattering coefficients for the specularly reflected radiation depending on the plate flutter: $\theta_1 = -40°$, $\varphi_1 = 0°$, $\theta_2 = 100°$, $\varphi_2 = 0°$, $\beta = 20°$, $\lambda = 0.694$ μm, $\tilde{n} = 1.31 + i\cdot10^{-3}$, $\mu = 5$: $N = 40$ liter^{-1}, $\overline{a} = 25$ μm (*1*); $N = 35$ liter^{-1}, $\overline{a} = 50$ μm (*2*); $N = 20$ liter^{-1}, $\overline{a} = 100$ μm (*3*); $N = 20$ liter^{-1}, $\overline{a} = 200$ μm (*4*).

The dependence of scattering coefficient on the angular characteristics, in particular, on the angle of light incidence onto a crystal and on the azimuth angle determining the orientation of the reference plane neglecting the particle flutter was illustrated in Ref. 10. It was shown that the changes of these angles lead to variations of the amplitude and polarization characteristics of the reflected radiation as well.

Figure 4 depicts the scattering coefficient $\beta_F(\theta_1)$ depending on the direction of sensing for different values of the flutter angle ψ. Note that for the illustrated $\beta_F(\theta_1)$ curves it is valid that $\theta_1 = \beta$. It can be seen from Fig. 4 that the curves are almost identical at small flutter values. Small fluctuations of the plates do not change the reflection features caused by different angles β, but only lead to an even decrease in the intensity of the specularly reflected radiation. It should be noted that this statement is true for both monostatic and bistatic sensing.

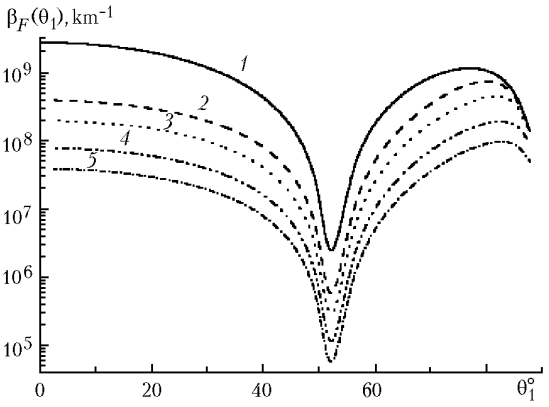

Fig. 4. Dependence of the scattering coefficient $\beta_F(\theta_1)$ for specularly reflected radiation at different values of the plate flutter angle: $\varphi_1 = 0°$, $\varphi_2 = 0°$, $\varphi_3 = 0°$, $\theta_2 = 180° - \theta_1$ ($\theta_1 = \beta$), $\theta_3 = 0°$, $\lambda = 0.694$ μm, $\tilde{n} = 1.31 + i\cdot10^{-3}$, $\mu = 5$, $N = 1$ liter^{-1}, $\overline{a} = 125$ μm: $\psi = 0°$ (*1*), 0.2° (*2*), 0.4° (*3*), 1° (*4*), 2° (*5*).

Note that the orientation of the polarization plane of incident radiation relative to the scatterer is uniquely related to the azimuth angle φ_1 (Refs. 7 and 11). Figures 5*a* and 5*b* show the numerically calculated data on, respectively, the scattering coefficient $\beta_F(\varphi_1)$ and the polarization characteristic $P_2 = \beta_{\pi_2}/\beta_{\pi_1}$ depending on the azimuth angle φ_1 for different values of the flutter ψ. The change of the incidence angle β (or θ_1) shifts the positions of the $\beta_F(\varphi_1)$ extremes. At the same values of φ_1, the larger ψ, the lower is the position of the $\beta_F(\varphi_1)$ maximum. For relatively high values of ψ (Fig. 5*a*, curve *6*) the dependence $\beta_F(\varphi_1)$ has an almost neutral behavior. The polarization characteristics vary only slightly at relatively small values of ψ (curves *1* and *2* in Fig. 5*b*), and only large flutter values lead to marked changes in $P_2(\varphi_1)$ (curves *1* and *4* or *5* and *7* in Fig. 5*b*).

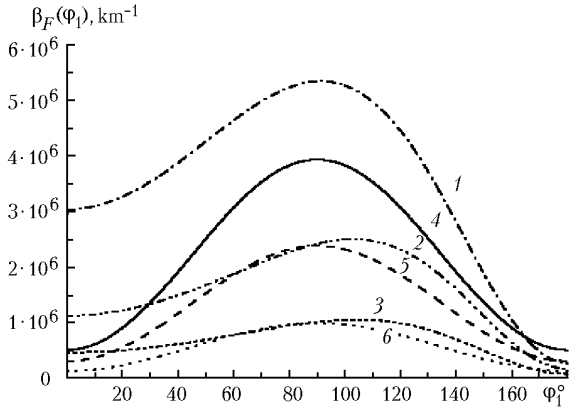

Fig. 5*a*. Dependence of the scattering coefficient $\beta_F(\varphi_1)$ for specularly reflected radiation at different values of the plate flutter: $\varphi_2 = 0°$, $\theta_2 = 100°$, $\lambda = 0.694$ μm, $\tilde{n} = 1.31 + i\cdot10^{-3}$, $\mu = 5$, $N = 1$ liter^{-1}, $\overline{a} = 25$ μm: $\psi = 0°$, $\theta_1 = -40°$ (*1*); $\psi = 0.4°$, $\theta_1 = -40°$ (*2*); $\psi = 1°$, $\theta_1 = -40°$ (*3*); $\psi = 0°$, $\theta_1 = 0°$ (*4*); $\psi = 0.4°$, $\theta_1 = 0°$ (*5*); $\psi = 1°$, $\theta_1 = 0°$ (*6*).

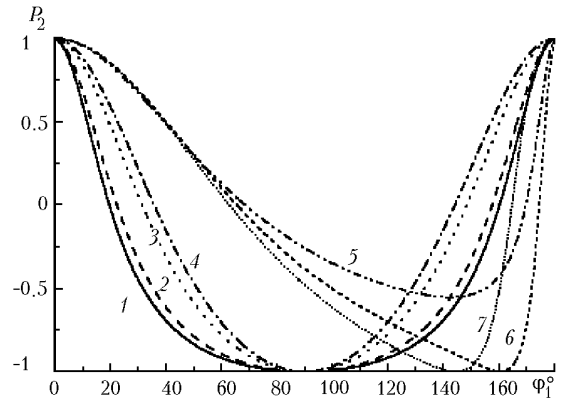

Fig. 5*b*. Dependence $P_2(\varphi_1)$ for specularly reflected radiation at different values of the flutter angle: $\varphi_2 = 0°$, $\theta_2 = 100°$, $\lambda = 0.694$ μm, $\tilde{n} = 1.31 + i\cdot10^{-3}$, $\mu = 5$, $N = 1$ liter^{-1}, $\overline{a} = 25$ μm: $\psi = 0°$, $\theta_1 = 0°$ (*1*); $\psi = 2°$, $\theta_1 = 0°$ (*2*); $\psi = 10°$, $\theta_1 = 0°$ (*3*); $\psi = 15°$, $\theta_1 = 0°$ (*4*); $\psi = 2°$, $\theta_1 = -40°$ (*5*); $\psi = 10°$, $\theta_1 = -40°$ (*6*); $\psi = 15°$, $\theta_1 = -40°$ (*7*).

In the experimental studies of abnormal backscattering, small values of the depolarization ratio of about 0.001–0.002 caused by small (less than 1°) flutter of the plates are observed, and in cloud layers that undergo stronger motion, where the flutter is about 10°, the depolarization is about 0.05–0.1 (Ref. 2).

Figure 6 depicts the spectral dependences of the coefficients $\beta_F(\lambda)$ at different values of the flutter ψ. To calculate the wavelength dependence of the scattering characteristics, let us use the dependences $n = n(\lambda)$ and $\chi = \chi(\lambda)$ drawn based on the data from Ref. 9. Obviously, the higher ψ, the smaller $\beta_F(\lambda)$. Notice that β_F nonlinearly depends on the ratio $\overline{a}/\lambda$.

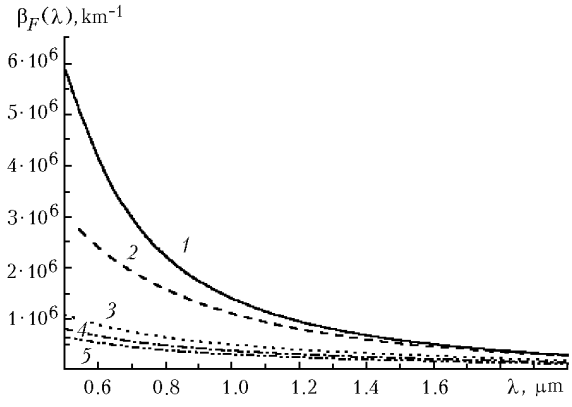

Fig. 6. Dependence of the scattering coefficient of specularly reflected radiation $\beta_F(\lambda)$ at different flutter angles: $\overline{a} = 25$ μm, $N = 1$ liter^{-1}, $\mu = 5$, $\varphi_1 = 0°$, $\varphi_2 = 0°$, $\theta_2 = 100°$, $\theta_1 = -40°$, $\beta = 20°$: $\psi = 0°$ (*1*), 0.2° (*2*), 0.6° (*3*), 0.8° (*4*), 1° (*5*).

The larger $\overline{a}$ and the smaller λ, the higher β_F. As was already mentioned (when discussing Fig. 3), the dependence of the scattering characteristics on small flutter angles manifests itself in the case of large

plates. It can be seen from Fig. 6 that small flutter values lead to the decrease in the intensity of the reflected signal within one order of magnitude, and these changes are characteristic of the visible and near IR regions. In the rest part of the IR region, $\beta_F(\lambda)$ curves for small ψ almost do not change.

The directivity of reflection for the system of fluttering ice plates also remain high, though decreases with increasing ψ. Scattering is almost isotropic within the 2ψ range, and beyond this range the intensity of the scattered field decreases sharply. This mechanism is described by curves *2*–*6* in Figs. 7 and 8.

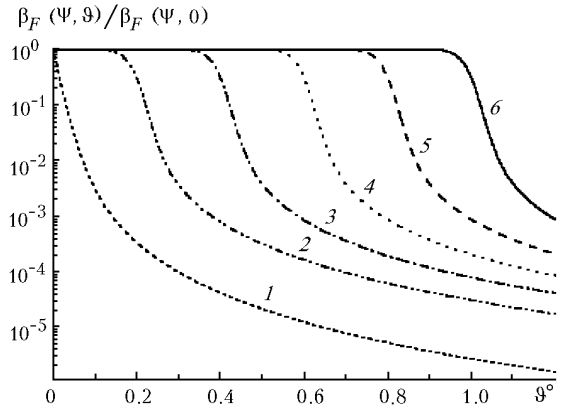

Fig. 7. Scattering coefficient ratio for specularly reflected radiation for a system of large fluttering plates ($\overline{a}$ = 200 μm) depending on the angle ϑ: $\varphi_1 = 0°$, $\theta_1 = -40°$, $\varphi_2 = 0°$, $\theta_2 = 100°$, $\beta = 20°$, $\lambda = 0.694$ μm, $N = 1$ liter^{-1}, $\mu = 5$, $\tilde{n} = 1.31 + i\cdot 10^{-3}$; $\psi = 0°$ (*1*), 0.2° (*2*), 0.4° (*3*), 0.6° (*4*), 0.8° (*5*), 1° (*6*).

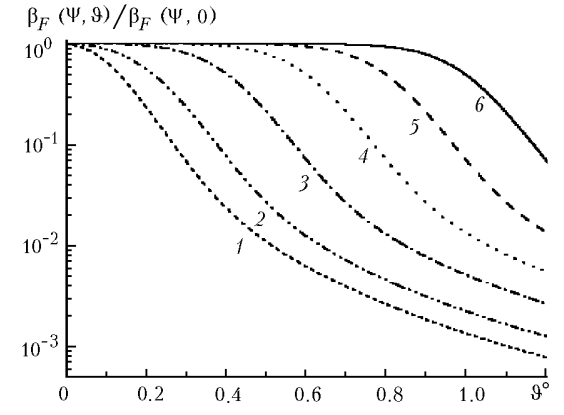

Fig. 8. Scattering coefficient ratio for specularly reflected radiation for a system of small fluttering plates ($\overline{a}$ = 25 μm) depending on the angle ϑ: $\varphi_1 = 0°$, $\theta_1 = -40°$, $\varphi_2 = 0°$, $\theta_2 = 100°$, $\beta = 20°$, $\lambda = 0.694$ μm, $N = 1$ liter^{-1}, $\mu = 5$, $\tilde{n} = 1.31 + i\cdot 10^{-3}$: $\psi = 0°$ (*1*), 0.2° (*2*), 0.4° (*3*), 0.6° (*4*), 0.8° (*5*), 1° (*6*).

For each dependence $\beta_F(\psi, \vartheta)/\beta_F(\psi, 0)$ the length of a horizontal range, within which scattering is isotropic, is determined by the flutter ψ. For relatively large plates (see Fig. 7) the flutter angle corresponds to halving of the reflected signal intensity at small-angle receiver (or source) scanning. However, this relation is violated for relatively small plates and small flutter (see Fig. 8). Notice that the steepness of the drop part is almost independent of the flutter, but it is determined by the mean size of plates. The dependences shown in Figs. 7 and 8 were calculated for $\beta = 20°$. It should be noted that this scattering feature is observed at any β, that is, for the case of specular reflection at monostatic and bistatic sensing.

Conclusion

Crystal clouds include ice plates, whose percentage is usually higher than that for other types of crystals. The intensity of the field specularly reflected from the plates with the allowance for their possible flutter significantly (by orders of magnitude) exceeds that for any other oriented crystals of extended shapes. Consequently, the model of a cloud as an ensemble of oriented fluttering plates that is proposed in this paper can be used for solution of the direct and inverse problems in monostatic and bistatic sensing of crystal clouds.

Analysis of numerically calculated scattering characteristics revealed the following. The plate flutter and the parameters of the particle size distribution, namely, the mean plate radius ($\overline{a}$) and the dimensionless parameter characterizing how steep are the slopes in the gamma distribution (μ) can be determined from estimated relative characteristics of specularly reflected radiation obtained at small-angle lidar scanning. Besides, the information content increases for the wavelengths in the visible region. From the results of relative measurements of the scattering coefficient, it is possible to estimate the flutter and the mean radius of plates. The refractive index and the position of the plates in space with respect to the source and receiver can be determined from the data on polarization characteristics of the reflected signal, which are almost independent of the small flutter angles and the parameters of the particle size distribution. With the known refractive index, it is possible to estimate the concentration of plates in the scattering volume from the absolute values of the refractive index.

Acknowledgments

The financial support from the Russian Foundation for Basic Research (Grant No. 01–05–65209) and the Ministry of Industry, Science, and Technologies of Russia (Grant "High-altitude polarization lidar" No. 06–21) is acknowledged.

References

1. M.I. Mischenko, J.W. Hovenier, and L.D. Travis, eds., *Light Scattering by Nonspherical Particles. Theory,*

Measurements, and Application (Academic Press, 2000), 690 pp.
2. C.M.R. Platt, J. Appl. Meteorol. **17**, No. 4, 482–488 (1978).
3. C.M.R. Platt, N.L. Abshire, and G.T. McNice, J. Appl. Meteorol. **17**, No. 8, 1220–1224 (1978).
4. J. Hallett, J. Opt. Soc. Am. A **4**, No. 3, 581–589 (1987).
5. B.M. Welsh and Ch.S. Gardner, Appl. Opt. **28**, No. 1, 32–82 (1989).
6. A.A. Popov and O.V. Shefer, J. Appl. Opt. **33**, No. 30, 7038–7044 (1994).
7. O.V. Shefer, Atmos. Oceanic Opt. **12**, No. 7, 549–553 (1999).
8. A.A. Popov and O.V. Shefer, Appl. Opt. **34**, No. 4, 1488–1492 (1995).
9. O.A. Volkovitskii, L.N. Pavlova, and A.G. Petrushin, *Optical Properties of Crystal Clouds* (Gidrometeoizdat, Leningrad, 1984), 200 pp.
10. O.V. Shefer, Atmos. Oceanic Opt. **15**, No. 10, 804–809 (2002).
11. O.V. Shefer, Atmos. Oceanic Opt. **14**, No. 8, 607–612 (2001).